UDS 621.382:539.3

OPTIMISATION OF PARAMETERS FOR LASER CLEAVING OF SILICATE GLASSES USING U-SHAPED BEAMS

YU. V. NIKITYUK, A. N. SERDYUKOV
Educational Institution "Francisk Skorina Gomel State University", the Republic of Belarus,

J. MA, L. WANG
Nanjing University of Science and Technology, China

I. YU. AUSHEV
State Educational Institution "University of Civil Protection of the Ministry for Emergency Situations of the Republic of Belarus, Minsk

Regression and neural network models to analyze the laser cleaving process of silicate glasses using U-shaped laser beams have been developed. The numerical experiment employed a central composite layout. The processing speed, laser beam power, and its geometrical parameters were chosen as variable factors. The values of maximum temperatures and maximum thermoelastic tensile stresses in the treatment zone were calculated as responses. The responses were determined via APDL (Ansys Parametric Design Language). Effective architectures for artificial neural networks have been established with TensorFlow in order determine the maximum temperatures and thermoelastic stresses in the laser-treated area. A comparison was conducted to assess the accuracy of neural network and regression models. The evaluation was performed to determine the impact of input parameters on the responses. The genetic algorithm of the DesignXplorer module was employed to ascertain the optimal modes for separating cracks formation in silicate glass though the use of U-shaped laser beams and a refrigerant.

Keywords: laser cleaving, artificial neural network, optimization, genetic algorithm, ANSYS.

ОПТИМИЗАЦИЯ ПАРАМЕТРОВ ЛАЗЕРНОГО РАСКАЛЫВАНИЯ СИЛИКАТНЫХ СТЕКОЛ U-ОБРАЗНЫМИ ПУЧКАМИ

Ю. В. НИКИТЮК, А. Н. СЕРДЮКОВ
Учреждение образования «Гомельский государственный университет имени Франциска Скорины», Республика Беларусь

Ц. МА, Л. ВАН
Нанкинский университет науки и технологий, Китайская Народная Республика

И. Ю. АУШЕВ
Государственное учреждение образования «Университет гражданской защиты Министерства по чрезвычайным ситуациям Республики Беларусь», г. Минск

Получены регрессионные и нейросетевые модели процесса лазерного раскалывания силикатных стекол U-образными лазерными пучками. Численный эксперимент выполнялся при помощи центрального композиционного плана. Скорость обработки, мощность лазерного пучка и его геометрические параметры были выбраны в качестве варьируемых факторов. Значения максимальных температур и максимальных термоупругих напряжений растяжения в зоне обработки вычислялись в качестве откликов. Определение откликов было выполнено с использованием языка программирования APDL. С использованием программы TensorFlow установлены эффективные архитектуры искусственных нейронных сетей для определения максимальных температур и максимальных термоупругих напряжений в зоне лазерной обработки. Выполнено сравнение точности нейросетевых и регрессионных моделей. Осуществлена оценка влияния входных параметров на отклики. С использованием генетического алгоритма модуля DesignXplorer определены оптимальные режимы формирования разделяющих трещин в силикатном стекле U-образными лазерными пучками и хладагентом.

Ключевые слова: лазерное раскалывание, искусственная нейронная сеть, оптимизация, генетический алгоритм, ANSYS.

Introduction

The extensive industrial use of silicate glass is due to its unique combination of properties. Cutting is a prominent procedure in the manufacturing of glass products, and laser cleaving technology offers notable advantages compared to conventional mechanical cutting methods. The advent of laser cleaving technology occurred throughout the latter half of the twentieth century. Research into the processes of cutting brittle non-metallic materials via laser cleaving methods is also of current relevance [1–12].

Controlled laser cleaving is a highly successful approach for cutting silicate glass. The standard approach for implementing controlled laser cleaving involves heating the surface of the material with a circular or elliptical laser beam. The surface is subsequently cooled by directing an air-water mixture onto the laser-heated region. This sequence of laser radiation and refrigerant exposure results in the formation of laser-induced cracks along the processing line and enables the qualitative separation of the material being processed [4].

In order to enhance the efficiency of this technology, it is feasible to employ laser beams with specific geometry, including U-shaped beams. The use of these beams guarantees the generation of sufficiently substantial values of tensile stresses within the material, while reducing the maximum temperature inside the treatment zone. This characteristic of heating by U-beams can be used in the processing of heat-sensitive materials. Furthermore, the use of U-shaped beams allows for reducing the effect of the processing contour proximity to the sample boundary on the development of a laser-induced crack [9].

In several instances of optimizing laser processing parameters, the use of metamodels has proven to be effective. These metamodels, employing regression and neural network models, enable the determination of output processing parameters without the need for complete calculations. In the subsequent phase of metamodeling, the use of genetic algorithms presents the potential to ascertain the optimal parameters for laser processing [13–17].

Using regression, neural network models, and a genetic algorithm, this paper investigates the process of laser cleaving of silicate glasses with U-shaped beams and identifies effective modes for generating laser-induced cracks.

Determination of optimal parameters of laser glass cutting

Temperatures and thermoelastic stresses produced in silicate glasses under the action of a U-shaped laser beam and a refrigerant were determined using APDL as part of the unrelated task of thermoelasticity in a quasi-static formulation.

Figure 1 illustrates the schematic of the spatial arrangement of the laser and refrigerant exposure areas.

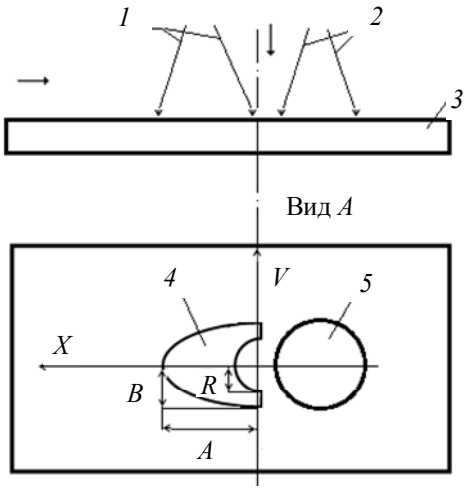

Fig. 1. Schematic of the spatial arrangement of the laser and refrigerant exposure area

Figure 1 illustrates the various positions within the experimental setup. Position *1* represents the laser beam with a wavelength of 10.6 microns, position *2* corresponds to the refrigerant, position *3* denotes the glass plate, position *4* indicates the cross-section of laser beam *1* in the cutting plane, and position *5* represents the cross-section of the refrigerant exposure in the cutting plane. The horizontal arrow indicates the movement direction of the glass plate with respect to the laser radiation.

The characteristics of silicate glasses employed in the calculations were specific heat capacity C = 860 J/kg · K; thermal conductivity λ = 0.88 W/m · K; density ρ = 450 kg/m^3; Young's modulus E = 70 Gpa; Poisson's ratio ν = 0.22, and thermal expansion coefficient $\alpha_T = 89 \cdot 10^{-7}$ (1/K) [2].

Finite element calculations were performed for a plate with dimensions of 0.025 × 0.02 × 0.002 m. The corresponding finite element model consisted of 27600 Solid 70 and Solid 185 elements utilized for thermal and strength analysis, respectively.

The calculations were performed using the following parameters: the processing speed V was set to 0.03 m/s, the laser power P was set to 10 W, the major semi-axis of the laser beam A was set to $8 \cdot 10^{-3}$ m, and the minor semi-axis B was set to $2 \cdot 10^{-3}$ m (Fig. 1).

The computed distributions of temperature fields and thermoelastic stress fields for the specified parameters of laser-induced heating of the silicate glass surface are provided in Fig. 2.

The maximum temperature for the calculated parameters did not exceed the glass transition temperature of the material being processed, which is equal to 789 K for silicate glass. This is a prerequisite for the implementation of laser cleaving [2].

The use of U-shaped beams does not lead to fundamental differences in the spatial distribution of tensile and compressive stress areas when compared to controlled laser cleaving using elliptical or circular laser beams [9]. Simultaneously, the use of U-shaped beams results in a decrease in maximum temperatures within the treatment zone, while ensuring that tensile stress values, which are created in the region where refrigerant is supplied, remain sufficiently high for the initiation and progression of a laser-induced crack.

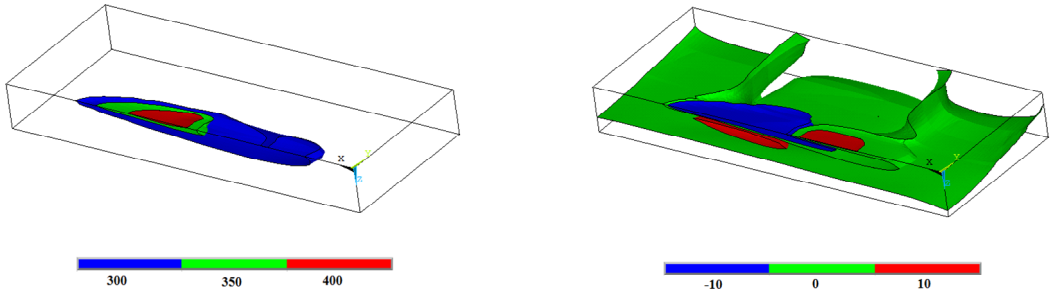

a) *b*)

Fig. 2. Computed distributions of temperatures, K (*a*) and stresses σ_{yy}, Mpa (*b*) when exposed to a U-shaped laser beam and a refrigerant

The numerical experiment was carried out using 27 combinations of the face-centered version of the central composite design for five factors (*P*1–*P*5): *P*1 was the processing speed *V*, *P*2 was the laser power *P*, *P*3 was the major semi-axis of the laser beam *A*, and *P*4 was the minor semi-axis of the beam *B*, *P*5 was the inner contour radius *R*. The following responses were determined: maximum temperature *T* and maximum tensile stresses σ_{yy} in the treatment zone (Table 1).

Table 1

Experimental design and calculation results

Number	*P*1 *V*, m/s	*P*2 *P*, W	*P*3 *A*, m	*P*4 *B*, m	*P*5 *R*, m	*P*6 *T*, K	*P*7 σ_{yy}, Mpa
1	0.02	20	0.008	0.004	0.002	479	17.5
2	0.01	20	0.008	0.004	0.002	556	33.8
3	0.03	20	0.008	0.004	0.002	443	11.0
4	0.02	10	0.008	0.004	0.002	386	8.7
5	0.02	30	0.008	0.004	0.002	572	26.2
6	0.02	20	0.006	0.004	0.002	511	15.1
7	0.02	20	0.01	0.004	0.002	460	17.7
8	0.02	20	0.008	0.003	0.002	545	28.2
9	0.02	20	0.008	0.005	0.002	447	12.1
10	0.02	20	0.008	0.004	0.001	479	18.1
11	0.02	20	0.008	0.004	0.003	492	18.6
12	0.01	10	0.006	0.003	0.003	558	31.0
13	0.03	10	0.006	0.003	0.001	403	8.3
14	0.01	30	0.006	0.003	0.001	878	73.4
15	0.03	30	0.006	0.003	0.003	714	30.4
16	0.01	10	0.01	0.003	0.001	447	27.1
17	0.03	10	0.01	0.003	0.003	398	9.7
18	0.01	30	0.01	0.003	0.003	847	94.7
19	0.03	30	0.01	0.003	0.001	558	24.6
20	0.01	10	0.006	0.005	0.001	416	11.6
21	0.03	10	0.006	0.005	0.003	372	3.4

Ending

Number	*P*1 *V*, m/s	*P*2 *P*, W	*P*3 *A*, m	*P*4 *B*, m	*P*5 *R*, m	*P*6 *T*, K	*P*7 σ_{yy}, Mpa
22	0.01	30	0.006	0.005	0.003	718	26.9
23	0.03	30	0.006	0.005	0.001	500	14.0
24	0.01	10	0.01	0.005	0.003	390	12.9
25	0.03	10	0.01	0.005	0.001	348	4.5
26	0.01	30	0.01	0.005	0.001	582	40.2
27	0.03	30	0.01	0.005	0.003	460	11.3

The resulting regression equations that establish the relationship between the response functions (T, σ_{yy}) and the factors (V, P, A, B, R) are as follows:

$$Y_T = 6.26 \cdot 10 - 7.41 \cdot 10^2 \cdot V + 1.46 \cdot P - 1.02 \cdot 10^4 \cdot B +$$

$$+ 1.16 \cdot 10^4 \cdot V \cdot V + 1.01 \cdot 10^6 \cdot B \cdot B + 4.43 \cdot 10^4 \cdot B \cdot B - 1.16 \cdot 10 \cdot V \cdot P +$$

$$+ 5.19 \cdot 10^4 \cdot V \cdot B - 3.41 \cdot 10 \cdot P \cdot A - 1.05 \cdot 10^2 \cdot P \cdot B + 1.76 \cdot 10^5 \cdot R \cdot B;$$

$$T = \left(Y_T \cdot 0.512 + 1\right)^{\left(\frac{1}{0.512}\right)} - 1;$$

$$Y_S = 5.82 \cdot 10 - 6.57 \cdot 10^2 \cdot V + 7.34 \cdot 10^{-1} \cdot P + 1.43 \cdot 10^3 \cdot A - 5.99 \cdot 10^3 \cdot B +$$

$$+ 7.59 \cdot 10^3 \cdot V \cdot V - 7.63 \cdot 10^{-3} \cdot P \cdot P - 1.339.38 \cdot 10^4 \cdot A \cdot A + 4.36 \cdot 10^5 \cdot B \cdot B +$$

$$+ 5.15 \cdot 10^5 \cdot R \cdot R - 1.45 \cdot 10^4 \cdot V \cdot A + 3.06 \cdot 10^4 \cdot V \cdot B - 1.73 \cdot 10 \cdot P \cdot B -$$

$$- 9.42 \cdot P \cdot R + 9.30 \cdot 10^4 \cdot A \cdot B + 6.64 \cdot 10^4 \cdot A \cdot R - 5.95 \cdot 10^5 \cdot B \cdot R;$$

$$\sigma_{yy} = (Y_S \cdot 0.11 + 1)^{\left(\frac{1}{0.11}\right)} - 1.$$

Figure 3 illustrates the assessment of the impact of the input parameters on the output parameters. Both responses are significantly influenced by the processing speed V, laser power P, and the value B of the minor semi-axis of the laser beam when implementing controlled laser cleaving with U-shaped beams. Simultaneously, the values of the maximum temperatures in the treatment zone T and the maximum tensile stresses σ_{yy} are found to be considerably less affected by the major semi-axis size of the beam A and the inner contour radius R.

Figure 4 shows the dependences of maximum temperatures T and maximum tensile stresses σ_{yy} in the treatment zone on the processing parameters.

The algorithm given in [15] was used to simulate the laser cleaving process of silicate glasses by U-shaped beams of networks using artificial neural networks. The data preparation for training and testing artificial neural networks was performed using the outcomes of a numerical experiment presented in Table 1. Furthermore, another 200 combinations of finite element calculations were added, along with the 27 combinations from the central compositional design of the numerical experiment.

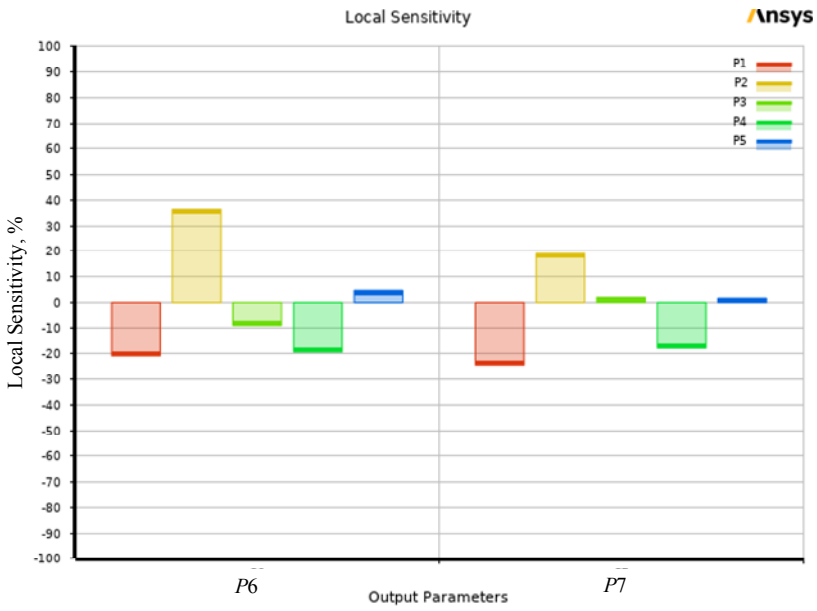

Fig. 3. Optimized parameter sensitivity chart:
*P*1 – *V*; *P*2 – *P*; *P*3 – *A*; *P*4 – *B*; *P*5 – *R*; *P*6 – *T*; *P*7 – σ_{yy}

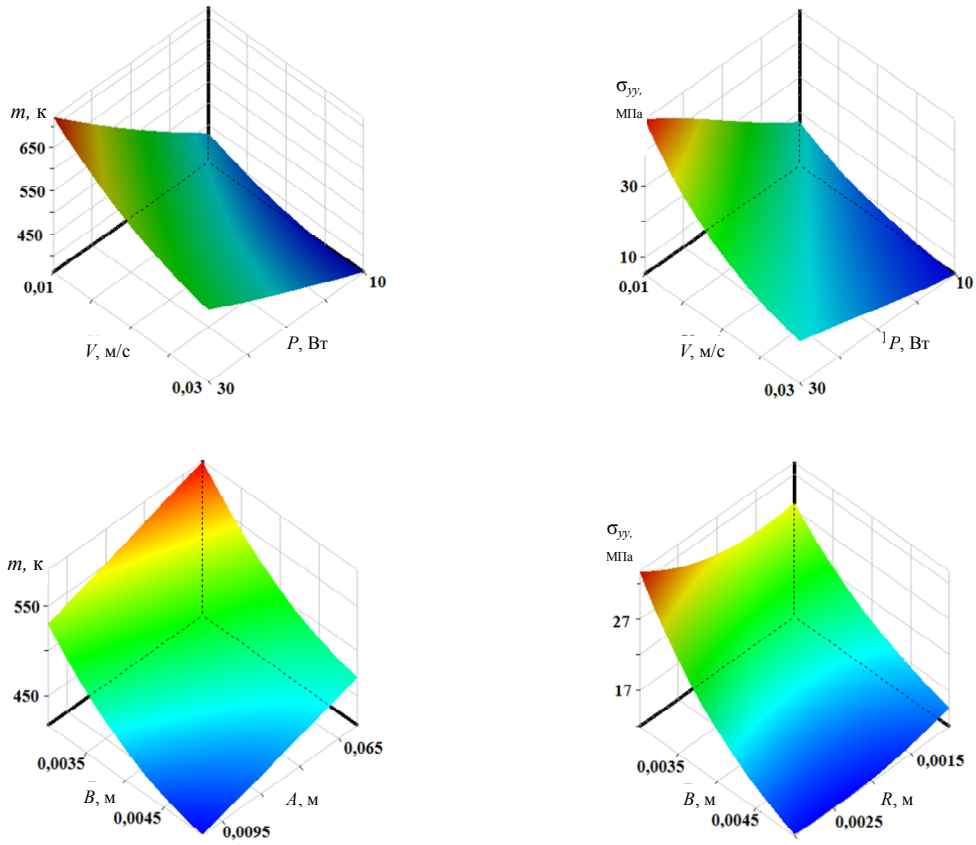

Fig. 4. Dependence of input parameters on output parameters

The construction of neural networks containing two hidden layers (Fig. 5) was performed using TensorFlow.

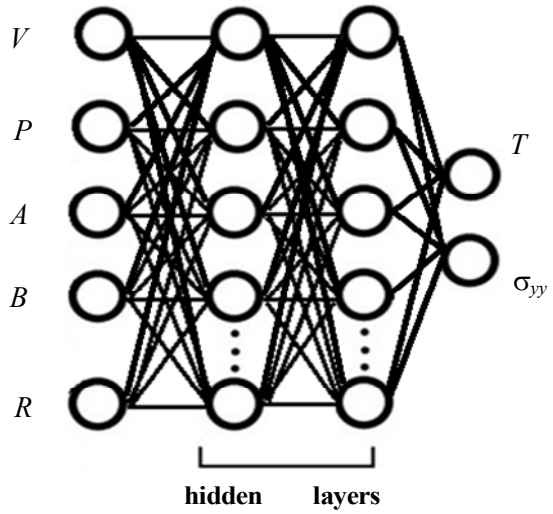

Fig. 5. Artificial neural network architecture

The Adam optimizer, ReLU activation function, and MSE loss function were applied in the process of constructing the artificial neural network. The neural network underwent training for a total of 500 epochs. Consequently, 16 artificial neural networks were created with the number of neurons in two hidden layers ranging from 5 to 20, with an interval of 5.

The dataset presented in Table 2 was used to perform tests on regression and neural network models.

Table 2

Test dataset

Number	*P*1 *V*, m/s	*P*2 *P*, W	*P*3 *A*, m	*P*4 *B*, m	*P*5 *R*, m	*P*6 *T*, K	*P*7 σ_{yy}, Mpa
1	0.018	14	0.007	0.003	0.003	538	25.9
2	0.018	30	0.009	0.005	0.002	522	21.1
3	0.014	23	0.006	0.004	0.002	595	24.8
4	0.016	26	0.008	0.003	0.002	661	45.9
5	0.013	24	0.008	0.003	0.001	652	50.6
6	0.029	24	0.008	0.004	0.003	487	14.4
7	0.014	17	0.009	0.004	0.003	486	23.6
8	0.01	18	0.006	0.003	0.002	660	43.7
9	0.012	20	0.01	0.004	0.002	509	30.2
10	0.03	23	0.01	0.004	0.002	448	12.3

The resulting models were evaluated using mean absolute error (*MAE*), root mean square error (*RMSE*), mean absolute percentage error (*MAPE*), and determination coefficient R^2 [15].

Figures 6–7 show heat maps illustrating the distribution of validation errors in determining the maximal values of temperature and tensile stresses in the treatment zone of silicate glasses using U-shaped beams. The number of neurons in the first and second hidden layers of the artificial neural network are shown by the vertical and horizontal axes,

especttively. The intensity of color coding represents the extent of error: the error increases from light to dark.

The artificial neural network with the architecture [5–5–20–2] demonstrated the most favourable results when determining the values of maximum temperatures T in the treatment zone. The artificial neural network with the architecture [5–15–15–2] produced the best results in determining the maximum tensile stresses σ_{yy} in the treatment zone.

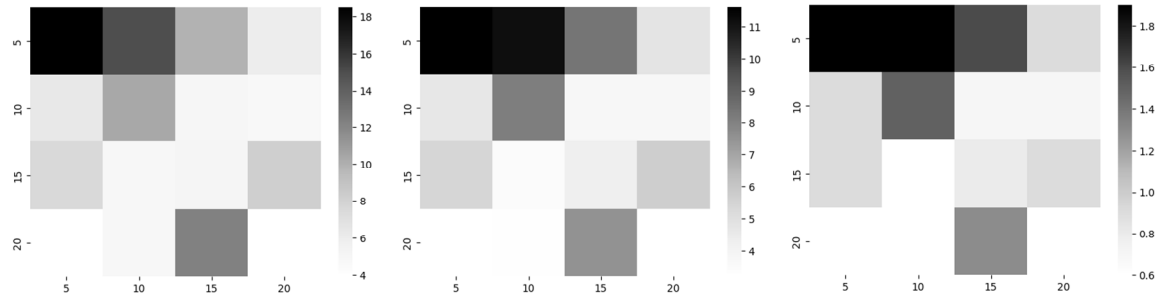

a) *b*) *c*)

Fig. 6. Heat maps of validation error distribution when determining T:
a – RMSE; *b – MAE*; *c – MAPE*

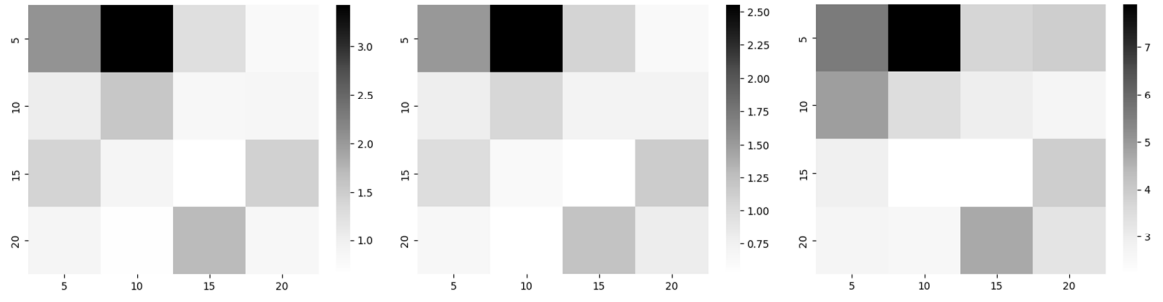

a) *b*) *c*)

Fig. 7. Heat maps of validation error distribution when determining σ_{yy}:
a – RMSE; *b – MAE*; *c – MAPE*

Table 3 displays the estimation outcomes of both the regression and neural network models.

Table 3

Evaluation results of regression and neural network models

Criterion	Regression model		Neural network model	
	T	σ_{yy}	T	σ_{yy}
RMSE	17.6 K	0.91 Mpa	3.9 K	0.65
MAE	13.2 K	0.75 Mpa	3.2 K	0.52
MAPE	2.3 %	2.6 %	0.6 %	2.2 %
R^2	0.9462	0.9949	0.9974	0.9973

The evaluation findings of the generated models indicate a required consistency with the outcomes obtained from finite element computations. The data in Table 3 show that

neural network models exhibit higher efficiency when it comes to predicting the output parameters of the controlled laser cleaving of silicate glasses using U-shaped beams.

The MOGA algorithm of the DesignXplorer module of the Ansys software was used to perform multicriteria optimization of parameters for controlled laser cleaving of silicate glass with U-shaped beams. The optimization procedures were conducted in accordance with the algorithm outlined in [16].

Using the DesignXplorer module, the following optimization criteria for controlled cleaving of silicate glass with U-shaped beams were chosen: $V \rightarrow \max$; $\sigma_{yy} \rightarrow \max$; $T \leq 789$ K.

Table 4 presents the optimization results. The response values calculated using APDL are provided in brackets.

Table 4

Optimization results

*P*1 *V*, m/s	*P*2 *P*, W	*P*3 *A*, m	*P*4 *B*, m	*P*5 *R*, m	*P*6 *T*, K	*P*7 σ_{yy}, Mpa
0.025	26.3	0.007	0.003	0.0025	632 (629)	29.4 (30.4)

The application of the MOGA algorithm ensured that the maximum relative error in determining the maximum temperatures and thermoelastic stresses did not exceed 1 % and 4 %, respectively.

Conclusion

This paper presents the construction of regression models of controlled laser cleaving of silicate glasses with U-shaped beams and determines the optimal neural network architectures, the accuracy of which was found to be superior to that of the corresponding regression models. The application of the MOGA algorithm in multicriteria optimization has led to the identification of modes for controlled laser cleaving of silicate glasses using U-shaped beams. These modes have been found to provide an increase in tensile stresses in the treatment zone compared to cleaving with circular or elliptical cross-section beams without an increase in the maximum temperatures in the sample. The parameters that have been determined ensure efficient generation of laser-induced cracks in silicate glasses.

References

1. Lumley R. M. Controlled separation of brittle materials using a laser. *Bjulleten' Amerikanskogo keramicheskogo obshhestva = American ceramic society bulletin*, 1969, vol. 48, pp. 850–854.
2. Machul'ka G. A. *Laser processing of glass.* Moscow, Sovetskoe radio Publ., 1979. 136 p.
3. Nisar S. Laser glass cutting techniques. *Zhurnal lazernyh prilozhenij = Journal of laser applications*, 2013, vol. 25, no. 4, pp. 042010-1–11.
4. Kondratenko V. S., Kudzh S. A. Precision Cutting of Glass and Other Brittle Materials by Laser-Controlled Thermo-Splitting. *Steklokeramika = Glass and ceramics*, 2017, no. 74, pp. 75–81. https://doi.org/10.1007/s10717-017-9932-1
5. Shalupaev S. V., Maksimenko A. V., Myshkovec V. N., Nikitjuk Ju. V. Laser cutting of ceramic materials with a metallized surface. *Zhurnal opticheskoj tehniki = Journal*

of Optical Technology, 2001, vol. 68, no. 10, pp. 758–760. ttps://doi.org/ 10.1364/JOT. 68000758

6. Shalupaev S. V., Shershnev E. B., Nikitjuk Ju. V., Sereda A. A. Two-beam laser thermal cleavage of brittle nonmetallic materials. *Zhurnal opticheskoj tehniki = Journal of Optical Technology*, 2006, vol. 73, no. 5, pp. 356–359. ttps://doi.org/ 10.1364/JOT. 73.000356
7. Shalupaev S. V., Serdjukov A. N., Mitjurich G. S., Aleksejuk M., Nikitjuk Ju. V., Sereda A. A. Modeling of mechanical influence of double-beam laser on single-crystalline silicon. *Arhiv metallurgii I materialov = Archives of Metallurgy and Materials*, 2013, vol. 58, no. 4, pp. 1381–1385. ttps://doi.org/10.2478/amm-2013-0179
8. Serdjukov A. N., Shalupaev S. V., Ju. V. Nikitjuk. Features of controlled laser thermal cleavage of crystalline silicon. *Crystallography Reports*, 2010, vol. 55, no. 6, pp. 933–937. ttps://doi.org/10.1134/S1063774510060064
9. Shalupaev S. V., Nikitjuk Ju. V., Sereda A. A., Aleksejuk M. The analysis of laser thermosplitting of fragile materials by using of special geometry beams. *Arhiv metallurgii I materialov* = Archives of Metallurgy and Materials, 2011, vol. 56, no. 4, pp. 1149–1155. ttps://doi.org/10.2478/v10172-011-0128-3
10. Serdjukov A. N., Shershnev E. B., Nikitjuk Ju. V., Sholoh V. F., Sokolov S. I. Features of controlled laser thermal cleavage of crystal quartz. *Crystallography Reports*, 2012, vol. 57, no. 6, pp. 792–797. ttps://doi.org/10.1134/S1063774512060120
11. Chzhao K., Chzhan H., Jan L., Van Ju., Din Ju. Dual laser beam revising the separation path technology of laser induced thermal-crack propagation for asymmetric linear cutting glass. *Mezhdunarodnyj zhurnal stankov I proizvodstva = International Journal of Machine Tools and Manufacture*, 2016, vol. 106, pp. 43–55. ttps://doi.org/10.1016/j.ijmachtools.2016.04.005
12. Wang H. L., Wang Y., Zhang H. Z., Wang X. W. Research Progress of Thermal Controlled Cracking of Hard-Brittle Plate. *Wuji Cailiao Xuebao*, 2018, vol. 33, no. 9, pp. 923–930. ttps://doi.org/10.15541/jim20170546
13. Parandoush, P., Hossain A. A review of modeling and simulation of laser beam machining. *Mezhdunarodnyj zhurnal stankov I proizvodstva = International Journal of Machine Tools and Manufacture*, 2014, no. 85, pp. 135–145.
14. Jiang P., Zhou Q., Shao X. *Surrogate model-based engineering design and optimization.* Singapore, Springer, 2020. 240 p. https://doi.org/10.1007/978-981-15-0731-1
15. Nikitjuk Ju. V., Serdjukov A. N., Aushev I. Ju. Determination of the parameters of two-beam laser splitting of silicate glasses using regression and neural network models. *Vestnik Belorusskogo gosudarstvennogo universiteta. Fizika = Journal of the Belarusian State University*. Physic, 2022, no. 1, pp. 35–43. ttps://doi.org/10.33581/2520-2243-2022-1-35-43
16. Nikitjuk Ju. V., Serdjukov A. N., Aushev I. Ju. Optimization of two-beam laser cleavage of silicate glass. *Zhurnal opticheskih tehnologij = Journal of Optical Technology,* 2022, vol. 89, no. 2, pp. 121–125. ttps://doi.org/10.1364/JOT.89.000121
17. Nikitjuk Ju. V., Sereda A. A., Serdjukov A. N., Shalupaev S. V., Aushev I. Ju. Parameters optimization of silicate glass two-beam asymmetric laser splitting. *Opticheskij zhurnal = Opticheskii Zhurnal*, 2023, vol. 90, no. 6, pp. 15–24. http://doi.org/10.-17586/1023-5086-2023-90-06-15-24

Поступила 02.10.2023